Organic Electronics 24 (2015) 263–271

Contents lists available at ScienceDirect

Organic Electronics

journal homepage: www.elsevier.com/locate/orgel

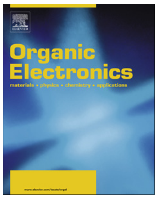

Polymer selection toward efficient polymer/PbSe planar heterojunction hybrid solar cells

Yaxiang Sun, Zeke Liu, Jianyu Yuan, Jianmei Chen, Yu Zhou, Xiaodong Huang, Wanli Ma *

Institute of Functional Nano & Soft Materials (FUNSOM) & Collaborative Innovation Center of Suzhou Nano Science and Technology, Soochow University, 199 Ren-Ai Road, Suzhou Industrial Park, Suzhou, Jiangsu 215123, China

ARTICLE INFO

Article history:
Received 2 April 2015
Received in revised form 21 May 2015
Accepted 3 June 2015
Available online 5 June 2015

Keywords:
Hybrid solar cells
Polymers
PbSe nanocrystals
Planar heterojunction
Morphology

ABSTRACT

By using a series of polymers in the polymer/PbSe planar heterojunction hybrid solar cells (HSCs), we found that the open circuit voltage of HSCs showed a great improvement compared to that of PbSe Schottky junction solar cells, which might be attributed to the formation of interface dipole, resulting in decreased interfacial resistance, increased built-in electrical field, as well as reduced exciton recombination at interface. Meanwhile, polymers with higher PL quenching have more favorable hole transfer which lead to better device performance. In addition, the energy levels and surface energy of the polymers might largely affect their interaction with PbSe NCs, leading to different interfacial morphologies and influencing the charge transfer efficiency. Furthermore, the optimized HSCs showed a remarkable PCE of 5.31% which was the highest efficiency reported for polymer/PbSe based HSCs. We believe this HSC efficiency can be further improved by selecting polymers with rationally designed structures.

1. Introduction

Polymer–colloidal nanocrystals (NCs) hybrid solar cells (HSCs) which combine the advantages of both organic and inorganic materials have attracted comprehensive research attention in recent years. Polymers can offer high absorbance coefficient and excellent film-forming ability while NCs may provide tunable bandgap across visible to near infrared (NIR) and high carrier mobility [1,2]. A variety of inorganic NCs have been studied in HSCs such as cadmium chalcogenides NCs (CdS [3,4], CdSe [5,6], CdTe [7,8]) and lead chalcogenides NCs (PbS [9–11], PbSe [12], PbSSe [13]). Compared to cadmium chalcogenides, PbS and PbSe have significant larger exciton Bohr radii (PbS 20 nm, PbSe 46 nm, CdSe 6 nm) [14] and hence demonstrate higher carrier mobility (PbSe 0.9–7 cm^{-2}V^{-1}S^{-1} [15–18], CdSe $\sim 10^{-2}$ cm^{-2}V^{-1}S^{-1} [19]) even without high temperature sintering. The bandgap of PbS and PbSe can be easily tuned to near infrared region to harvest low energy photons benefiting from their strong quantum confinement effect. In addition, PbSe quantum dots solar cells demonstrated multiple exciton generation (MEG) effect and a peak external quantum efficiency (EQE) as high as 114% was achieved [20]. So HSCs employing lead chalcogenides NCs and conjugated polymers show a great prospect in the full-spectrum photovoltaics.

In recent years, CdSe/polymer HSCs have been widely reported owing to the mature synthesis process and easy shape control of CdSe NCs which can work efficiently with many low band-gap polymers such as the commonly used conjugated polymer poly(3-hexylthiophene) (P3HT) [21,22], poly[2,6-(4,4-bis(2-ethylhexyl)-4H-cyclopenta[2,1-b;3,4-b']dithiophene)-alt-4,7-(2,1,3-benzothiadiazole)] (PCPDTBT) [5,23] poly(p-phenylenvinylene) derivative (OC$_1$C$_{10}$-PPV) [24], poly(2-methoxy-5-(2′-ethyl-hexyloxy)-1,4-phenylene vinylene) (MEH-PPV) [25]. In contrast, HSCs based on PbS or PbSe NCs have been far less investigated, with the PCE less than 1% for many years [26]. Recently, Prasad et al. used a low band-gap polymer poly(2,6-(N-(1-octylnonyl)dithieno[3,2-b:20,30-d]pyrrole)-alt-4,7-(2,1,3-benzothiadiazole)) (PDTPBT) [27] together with PbS NCs in HSCs which exhibited a high PCE of 3.78% [11]. Then we demonstrated a record-high PCE of 5.50% and a FF of 67% for HSCs using PDTPBT and PbS$_x$Se$_{1-x}$ alloy NCs [13]. However, to date only very limited polymers show good compatibility with lead chalcogenides in HSCs [11,28] and the performance of HSCs has still lagged significantly behind polymer/fullerene solar cells. It is very surprising since lead chalcogenide NCs possess remarkable photovoltaic properties as aforementioned. *What have limited the performance of polymer/PbS(PbSe) HSCs*? This important and fundamental question has, however, remained unsolved for many years. Thus to realize the full potential of NCs, it is critical to understand the hidden mechanisms which govern the interaction between polymers and NCs, and clarify the factors which determine the device performance. It is apparent that the selection of appropriate polymer is most essential

---

* Corresponding author.
E-mail address: wlma@suda.edu.cn (W. Ma).

http://dx.doi.org/10.1016/j.orgel.2015.06.010
1566-1199/© 2015 Elsevier B.V. All rights reserved.

in PbS(PbSe)/polymer HSCs since polymers with different properties can greatly impact the device performance. Herein, more polymers with rationally designed structures and fine tuned properties should be investigated to locate the most important properties and eventually reveal the possible polymer selection criteria for such HSCs.

In this work, a series of semiconducting polymers with the same donor comonomer cyclopenta[2,1-b:3,4-b]dithiophene (DTC) were investigated. DTC was used because it has proven successful as building block for PDTPBT in efficient PDTPBT/PbS HSCs [27]. The polymer properties were finely tuned by using different acceptor comonomers. PbSe NCs were used in HSCs since they have superior properties and are far less studied compared to PbS NCs [29,30]. It is worth noting that we adopted a simple planar-junction structure (PHJ) ITO/PEDOT/Polymer/PbSe/LiF/Al for polymer/PbSe HSCs, while the conventional HSCs use bulk-heterojunctions (BHJ) structure which involves complicated phase segregation between the mixed active materials [13]. Thus by using PHJ structure, we can largely simplify the device morphology and better find the correlation between photovoltaic performance and polymer properties by limiting the possible affecting factors. This is the first systematical study on the effect of different polymer structures on the photovoltaic parameters of PHJ hybrid devices based on lead chalcogenide NCs. We found that the V_{oc} of HSCs showed a great improvement compared to that of PbSe Schottky junction solar cells, which might be attributed to the formation of interface dipole, resulting in decreased interfacial resistance, increased built-in electrical field, as well as reduced exciton recombination at interface. In addition, the energy levels and surface energy of the polymers might largely affect their interaction with PbSe NCs, leading to different interfacial morphologies and influencing the charge transfer efficiency. Furthermore, the optimized HSCs showed a remarkable PCE of 5.31% which was the highest efficiency reported for polymer/PbSe based HSCs. We believe this HSC efficiency can be further improved by selecting polymers with rationally designed structures.

2. Experimental section

2.1. Nanocrystal synthesis

Nanocrystal synthesis was performed with a modified recipe previously documented. All operations were under nitrogen atmosphere using standard air-free Schlenk line techniques. A solution of 446 mg of PbO (2 mmol), 1.4 g of oleic acid (5 mmol), and 20 g of ODE was degassed at 100 °C in a 100 ml three-neck flask for 1 h under vacuum. The solution was then heated for an additional 1 h to 150 °C under nitrogen. After adjusting the solution to a desired temperature, 125 μl of $(TMS)_2Se$ (0.5 mmol) in 5 ml of ODE was rapidly injected into the hot solution. The NCs were grown at the desired temperature for an optimal time (10 min, 5 min, 2 min, 1.5 min, 1 min, 0.5 min for 80 °C 100 °C, 120 °C, 140 °C, 160 °C, 180 °C respectively), and the reaction was rapidly quenched by placing the flask in a room-temperature water bath and injecting 8 ml of anhydrous hexane, then purified by precipitation twice in hexane/isopropyl alcohol and once in hexane/acetone and stored with solid form in an nitrogen-filled glovebox.

2.2. Device fabrication and testing

The hybrid solar cells was fabricated with a common structure: ITO/PEDOT:PSS/Polymer/PbSe/LiF/Al. The ITO glass substrate was firstly cleaned by sequential ultrasonic treatment in detergent, isopropyl alcohol, acetone, A thin layer of PEDOT was deposited with 4500 rpm onto it and then thermally annealed at 150 °C for 10 min. 1 mg/ml Polymer dissolved in chloroform was spinning-coated onto the PEDOT film to form the polymer layer. Layer-by-layer (LBL) spin-coating was employed to fabricate the CQD film. Four thin NC layers with 40 mg/ml PbSe solution dissolved in hexane were deposited onto the polymer layer at 1500 rpm for 20 s. Post ligand-exchange was carried out: the film was soaked in a solution of 0.001 M BDT in acetonitrile for 10 s, then two rinsing steps with pure acetonitrile were performed to remove the excess of BDT and OA. The device was then dried at 100 °C for 10 min in glovebox. Finally, the device was loaded into the evaporation chamber, a 0.7 nm LiF (0.1 Å S^{-1}) and 100 nm Al (1 Å S^{-1} for the first 10 nm and 3 Å S^{-1} for the remaining 90 nm) were thermally evaporated at a pressure of 1×10^{-6} mbar through a shadow mask (active area 7.25 mm^2). The current density–voltage characteristics of the photovoltaic cells were measured using a Kheithey 2400 (*I–V*) digital source meter under a simulated AM 1.5G solar irradiation at 100 mW/cm^2 (Newport, Class AAA solar simulator, 94023A-U). The light intensity is calibrated by a certified Oriel Reference Cell (91150V) and verified with a NREL calibrated Hamamatsu S1787-04 diode.

2.3. Characterization

UV–Vis–NIR spectra were recorded on a Perkin Elmer model Lambda 750. Capacitance–voltage (*C–V*) measurements were performed using an precision impedance analyzer 6500B series under C-R model, all measurements were performed in the dark. Surface potential mapping was performed in air by peak force amplitude modulation SKPM using an Dimension Icon atomic force microscope from Bruker. Transmission electron microscopy (TEM) images were obtained using a Tecnai G2 F20 S-Twin transmission electron microscope. TEM samples were prepared by spin-casting 1 mg/ml polymer solution dissolved in chloroform respectively on the PEDOT:PSS coated ITO, and then 10 mg/ml, 20 mg/ml, 40 mg/ml PbSe solution dissolved in n-hexane was respectively deposited onto the polymer film, ligand exchanged with BDT, then thermal annealing at 100 °C for 10 min. During the lift-off process, the spin-coated films were pre-cut into several small pieces and rinsed in water, the films were then transferred to pure copper grids without carbon membrane for test. The PL intensity measurement was performed by HORIB-FM-2015. The scanning electron microscopy (SEM) operating were performed on a Zeiss Supra 55 field in high vacuum mode at 10 kV accelerating voltages. The UPS measurement was performed in an Omicron Nanotechnology system with a base pressure of 2×10^{-10} Torr.

3. Results and discussion

3.1. Solar cell performance

PbSe NCs with different bandgaps were synthesized according to our previous report [30]. The absorbance spectra of PbSe NCs with the reaction temperature from 80 °C to 180 °C are shown in Fig. 1a, with the insert showing the monodispersed NCs synthesized at 140 °C. Fig. 1b shows the apparent bandgap tuning effect by adjusting synthesis temperature, due to the extremely strong quantum confinement of PbSe NCs. The valence bands (VB) of these NCs were measured by ultraviolet photoelectron spectroscopy (UPS) (Fig. S1) and summarized in Fig. 2a together with their calculated conduction bands (CB). Meanwhile, A series of polymers PDTPBT [27], PDTD [31], PDBF [31], PDTT [31], P3HT [31], PDFT [31], PBDT-T-FDP [32], PBDTTPD [33], PBDT-T8-TPD [34] were also synthesized, with the structures shown in the Supplementary Information. Fig. S2. The HOMO levels of the polymers were